AXIAL DISPERSION FLOW IN TRICKLE BED REACTOR

[1]D. Bártová, [1]B. Jakeš, [2]V. Jiřičný, [1]J. Kukal, [2]V. Staněk, [2]P. Stavárek

[1] Institute of Chemical Technology, Department of Computing and Control Engineering,

[2]Institute of Chemical Process Fundamentals v.v.i., Dep. of Separation Processes, Academy of Sciences of the Czech Republic

Abstract

Evaluation of axial dispersion flow parameters in trickle bed reactor (TBR) as a identification task is studied in this paper. Four axial dispersion models (ADMs) were employed to identify principal flow parameters from experimental data. The impulse-response method was employed to measure the residence time distribution (RTD) in the liquid phase. Isobutanol was chosen as a tracer for the selected liquid phase represented by toluene. Tracer concentration at the outlet from the reactor was continuously monitored by a digital refractometer. Optimal model and the best predictions of the parameters were obtained via non-linear regression and least square method.

1 Introduction

Trickle bed reactors (TBRs) are randomly packed tubular devices employed in industrial 3-phase catalytic processes. The most widely used operation is downflow, where gas and liquid flows co-currently through packing in line with gravitational force. Thanks to simple construction and low operation costs are TBRs widely used in many industrial areas. Some examples of their applications are hydrocracking, hydrodesulfurization, hydrodenitrogenation in petroleum industry, hydrogenation in industry of petrochemicals and in wastewater treatment industry [1, 2].

In spite of many advantages of using TBRs, their most important disadvantage is non-uniform liquid flow through packing layer which has almost stochastic character. Due to this non-uniformities of liquid flow the catalyst surface may be incompletely wetted what results in low catalyst surface utilization. One of experimental methods commonly used for liquid flow characterization is measurement residence time distribution (RTD). With appropriate evaluation of such experimental data a useful properties of liquid flow structure can be found. The most important characteristics influencing reactant conversion and selectivity are the mean residence time of liquid phase and extent of back-mixing.

Even if TBRs were intensively studied in the past, unfortunately the most studies were conducted in laboratory reactors with air, water and nonporous particles, what is useless for industrial applications.

This paper is devoted to characterize liquid flow in trickle bed reactor with appropriate mathematical model based on experimental data of residence time distribution of organic liquid. Four mathematical models with axial dispersion with different boundary conditions were used.

2 Axial dispersion models

One of the main models which are used in chemical engineering praxis for the dynamic description of the behavior flow distributed parameter systems is an axial dispersion model (alias axial diffusion model). The diffusion in it is superimposed on plug flow. The general mathematical expression for this one-parametric model is a linear partial differential equation

$$\frac{\partial \mathrm{c}(x,t)}{\partial t} = D_{\mathrm{L}} \frac{\partial^2 \mathrm{c}(x,t)}{\partial x^2} - u \frac{\partial \mathrm{c}(x,t)}{\partial x}, \quad t > 0 \tag{1}$$

where by means tracer technique $\mathrm{c}(x, t)$ as a function of space coordinate and time is a concentration profile of the injected tracer in the exit stream of the canal, u is an average fluid velocity. The coefficient of axial dispersion D_{L} is a parameter of a model. It is also called turbulent diffusion coefficient or back mixing coefficient. Suppose the uniform intensity back mixing is the unique characteristic. This coefficient can be defined as

$$D_L = \lim_{\Delta x \to 0} u_b \Delta x \quad (m^2 s^{-1}) \tag{2}$$

where u_b is the velocity of back flow (m s^{-1}).

As a model parameter is more often used the dimensionless so called Peclet number *Pe* which is defined as

$$Pe = \frac{u\,H}{D_L} \tag{3}$$

where *H* is the real canal length.

The form of the solution and behavior of the model (see Eq. 1) then depends on the one initial and two boundary conditions. The four variants of these conditions are considered in this paper (see Table 1).

Table 1: THE INITIAL AND BOUNDARY CONDITIONS OF 4 CONSIDERED ADMS

ACC –	axial closed-closed model:	zero initial condition, closed canal, Danckwerts boundary conditions
ACO –	axial closed-open model:	zero initial condition, semi-closed canal, Danckwerts boundary condition for left part, zero boundary condition for right part of canal
AEO –	axial enforced closed-open model:	zero initial condition, semi-closed canal, enforced boundary condition in left closed part, zero boundary condition in right open and infinite part of canal
AOO –	axial open-open model:	zero initial condition, enforced condition in $x = 0$, infinite canal in both parts, zero boundary conditions

Eq. 1 was solved via one sided Laplace transform for selected initial and boundary conditions. The transfer functions G(*H*, *p*) were derived and the impulse (weighting) functions g(*H*, *t*) and step responses h(*H*, *t*) were obtained via inverse Laplace transform, operator rules and by using Laplace transform table for these ADMs.

For practical using, it is useful to express these functions as function of dimensionless time $\theta = t/\tau$, where the following relations are valid

$$\mathrm{g}(H,t) = \frac{1}{\tau}\mathrm{g}(H,\theta), \quad \mathrm{h}(H,t) = \mathrm{h}(H,\theta) \tag{4}$$

and where

$$\tau = M_1^t \tag{5}$$

is a dimensional 1st raw moment of g(*H*, *t*).

It is possible to obtain the mode by analytical solving of the following equation for the majority of the models discussed as

$$\frac{\mathrm{dg}(\theta)}{\mathrm{d}\theta} = 0 \quad \Rightarrow \quad \theta_M \tag{6}$$

By substituting the value obtained in the relation for the weighting function the value of the functional value of impulse function in mode $\mathrm{g}(\theta_M)$ is also calculated. The ACC model is once more an exception because the analytical expression for θ_M and $\mathrm{g}(\theta_M)$ is not available. The values can be obtained only via numerical calculation depending on Peclet number value.

The main properties of the four ADMs are presented in Tables 2-5. Some of these properties are useful for the parameter identification applied for the experimental data obtained from TBR.

Table 2: AXIAL ENFORCED CLOSED-OPEN MODEL PROPERTIES (AEO)

Item	Basic characteristics	Equation
a	Basic equation	$D_{\mathrm{L}}\dfrac{\partial^2 \mathrm{c}(x,t)}{\partial x^2} - u\dfrac{\partial \mathrm{c}(x,t)}{\partial x} = \dfrac{\partial \mathrm{c}(x,t)}{\partial t}$
b	Initial and boundary conditions	$\mathrm{c}(x,0) = 0,\ 0 \le x \le \infty$ $x = 0:\quad \mathrm{c}_{\mathrm{in}}(t) = \mathrm{c}(0,t)$ $x \to \infty : \mathrm{c}(\infty,t) = 0,\ t \ge 0$
c	Transfer function	$\mathrm{G}(H,p) = \exp\left(\dfrac{Pe}{2}(1-a)\right),\quad a = \sqrt{1+\dfrac{4p\tau}{Pe}},\quad \tau = H/u$
d	Impulse function (IF)	$\mathrm{g}(H,\theta) = \dfrac{1}{2\theta}\sqrt{\dfrac{Pe}{\pi\theta}}\exp\left(-\dfrac{Pe(1-\theta)^2}{4\theta}\right)$
e	Step response	$\mathrm{h}(H,\theta) = \dfrac{1}{2}\left[\mathrm{erfc}\left(\sqrt{\dfrac{Pe}{\theta}}\dfrac{1-\theta}{2}\right) + \mathrm{e}^{Pe}\,\mathrm{erfc}\left(\sqrt{\dfrac{Pe}{\theta}}\dfrac{1+\theta}{2}\right)\right]$
f	0^{th} raw moment of IF	$M_0^{\theta} = 1$
g	1^{st} raw moment of IF	$M_1^{\theta} = 1$
h	2^{nd} raw moment of IF	$M_2^{\theta} = 1 + 2/Pe$
i	3^{rd} raw moment of IF	$M_3^{\theta} = 1 + 6/Pe + 12/Pe^2$
j	4^{th} raw moment of IF	$M_4^{\theta} = 1 + 12/Pe + 60/Pe^2 + 120/Pe^3$
k	Dispersion, variance	$\sigma^2 = 2/Pe$
l	Coefficient of variation	$\gamma = \sqrt{2/Pe}$
m	Skewness	$\gamma_1 = 3\sqrt{2/Pe}$
n	Kurtosis	$\gamma_2 = 30/Pe$
o	Mode	$\theta_{\mathrm{M}} = (-3+b)/Pe,\quad b = \sqrt{9+Pe^2}$
p	Maximum of IF	$\mathrm{g}(H,\theta_{\mathrm{M}}) = \dfrac{Pe^2}{2\sqrt{\pi}\sqrt{(b-3)^3}}\exp\left(\dfrac{Pe-b}{2}\right)$

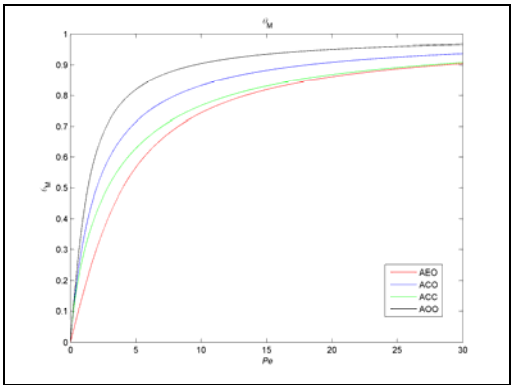

Figure 1: The dependence of θ_{M} on *Pe* for 4 models

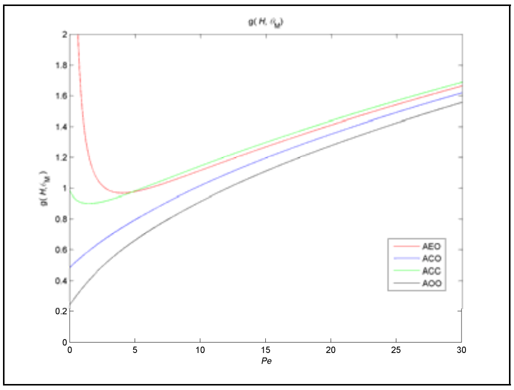

Figure 2: The dependence of $\mathrm{g}(H, \theta_{\mathrm{M}})$ on *Pe* for 4 models

Table 3: AXIAL CLOSED-CLOSED MODEL PROPERTIES (ACC)

Item	**Basic characteristics**	**Equation**
a	Basic equation	$D_{\mathrm{L}} \frac{\partial^2 \mathrm{c}(x,t)}{\partial x^2} - u \frac{\partial \mathrm{c}(x,t)}{\partial x} = \frac{\partial \mathrm{c}(x,t)}{\partial t}$
b	Initial and boundary conditions	$\mathrm{c}(x,0) = 0,\ 0 \le x \le H$ $x = 0: \quad \mathrm{c}_{\mathrm{in}}(t) = \mathrm{c}(0,t) - \frac{D_{\mathrm{L}}}{u} \frac{\partial \mathrm{c}(0,t)}{\partial x}$ $x = H: \ \left.\frac{\partial \mathrm{c}(0,t)}{\partial x}\right\|_{x=H} = 0$
c	Transfer function	$\mathrm{G}(H,p) = \exp(Pe/2)\left[\frac{1+a^2}{2a}\sinh\left(\frac{Pe}{2}a\right) + \cosh\left(\frac{Pe}{2}a\right)\right]^{-1},$ $a = \sqrt{1 + \frac{4p\tau}{Pe}}, \quad \tau = H/u$
d	Impulse function (IF)	$\mathrm{g}(H,\theta) = 2Pe\,\mathrm{e}^{0.5Pe} \sum_{k=1}^{\infty} \frac{(-1)^{k+1} \kappa_k^{\,2}}{4 + Pe(1+\kappa_k^{\,2})} \mathrm{e}^{q_k \theta},$ $q_k = p_k \tau, \quad p_k = -\frac{Pe(1+\kappa_k^{\,2})}{4\tau}$
e	Step response	$\mathrm{h}(H,\theta) = 1 + 8\,\mathrm{e}^{0.5Pe} \sum_{k=1}^{\infty} \frac{(-1)^k \kappa_k^{\,2}}{(1+\kappa_k^{\,2})(4 + Pe(1+\kappa_k^{\,2}))} \mathrm{e}^{q_k \theta}$
f	0^{th} raw moment of IF	$M_0^{\theta} = 1$
g	1^{st} raw moment of IF	$M_1^{\theta} = 1$
h	2^{nd} raw moment of IF	$M_2^{\theta} = 1 + 2/Pe - 2(1 - \mathrm{e}^{-Pe})/Pe^2$
i	3^{rd} raw moment of IF	$M_3^{\theta} = 1 + 6/Pe + 6(1 + 3\,\mathrm{e}^{-Pe})/Pe^2 - 24(1 - \mathrm{e}^{-Pe})/Pe^3$
j	4^{th} raw moment of IF	$M_4^{\theta} = 1 + 12/Pe + 12(4 + 9\,\mathrm{e}^{-Pe})/Pe^2 - 24(14 - 13\,\mathrm{e}^{-Pe})/Pe^4 +$ $+ 360\,\mathrm{e}^{-Pe}/Pe^3 + 24\,\mathrm{e}^{-2Pe}/Pe^4$
k	Dispersion, variance	$\sigma^2 = \frac{2(Pe - 1 + \mathrm{e}^{-Pe})}{Pe^2}$
l	Coefficient of variation	$\gamma = \frac{\sqrt{2(Pe - 1 + \mathrm{e}^{-Pe})}}{Pe}$
m	Skewness	$\gamma_1 = 3\sqrt{2}\frac{Pe - 2 + (Pe+2)\mathrm{e}^{-Pe}}{\sqrt{(Pe - 1 + \mathrm{e}^{-Pe})^3}}$
n	Kurtosis	$\gamma_2 = \frac{30Pe - 87 + 12Pe^2\mathrm{e}^{-Pe} + 60Pe\,\mathrm{e}^{-Pe} + 84\mathrm{e}^{-Pe} + 3\mathrm{e}^{-2Pe}}{(Pe - 1 + \mathrm{e}^{-Pe})^2}$
o	Mode	See Fig. 1
p	Maximum of IF	See Fig. 2

Table 4: AXIAL CLOSED-OPEN MODEL PROPERTIES (ACO)

Item	Basic characteristics	Equation
a	Basic equation	$D_{\mathrm{L}}\dfrac{\partial^2 \mathrm{c}(x,t)}{\partial x^2}-u\dfrac{\partial \mathrm{c}(x,t)}{\partial x}=\dfrac{\partial \mathrm{c}(x,t)}{\partial t}$
b	Initial and boundary conditions	$\mathrm{c}(x,0)=0, \quad 0\le x\le\infty$ $x=0: \quad \mathrm{c}_{\mathrm{in}}(t)=\mathrm{c}(0,t)-\dfrac{D_{\mathrm{L}}}{u}\dfrac{\partial \mathrm{c}(0,t)}{\partial x}$ $x\to\infty: \quad \mathrm{c}(\infty,t)=0$
c	Transfer function	$\mathrm{G}(H,p)=\dfrac{2\exp(0.5Pe(1-a))}{1+a}, \quad \tau=H/u, \quad a=\sqrt{1+\dfrac{4p\tau}{Pe}}$
d	Impulse function (IF)	$\mathrm{g}(H,\theta)=\sqrt{\dfrac{Pe}{\pi\theta}}\exp\left(-\dfrac{Pe(1-\theta)^2}{4\theta}\right)-\dfrac{Pe}{2}\mathrm{e}^{Pe}\,\mathrm{erfc}\left(\dfrac{\sqrt{Pe}(1+\theta)}{2\sqrt{\theta}}\right)$
e	Step response	$\mathrm{h}(H,\theta)=\sqrt{\dfrac{Pe\theta}{\pi}}\exp\left(-\dfrac{Pe(1-\theta)^2}{4\theta}\right)+\dfrac{1}{2}\mathrm{erfc}\left(\dfrac{\sqrt{Pe}(1-\theta)}{2\sqrt{\theta}}\right)-$ $-\dfrac{1}{2}(1+Pe+Pe\theta)\mathrm{e}^{Pe}\,\mathrm{erfc}\left(\dfrac{\sqrt{Pe}(1+\theta)}{2\sqrt{\theta}}\right)$
f	0^{th} raw moment of IF	$M_0^{\theta}=1$
g	1^{st} raw moment of IF	$M_1^{\theta}=1+1/Pe$
h	2^{nd} raw moment of IF	$M_2^{\theta}=1+4/Pe+4/Pe^2$
i	3^{rd} raw moment of IF	$M_3^{\theta}=1+9/Pe+30/Pe^2+30/Pe^3$
j	4^{th} raw moment of IF	$M_4^{\theta}=1+16/Pe+108/Pe^2+336/Pe^3+336/Pe^4$
k	Dispersion, variance	$\sigma^2=2/Pe+3/Pe^2$
l	Coefficient of variation	$\gamma=\dfrac{\sqrt{2Pe+3}}{Pe+1}$
m	Skewness	$\gamma_1=\dfrac{12Pe+20}{\sqrt{(2Pe+3)^3}}$
n	Kurtosis	$\gamma_2=\dfrac{120Pe+210}{(2Pe+3)^2}$
o	Mode	$\theta_{\mathrm{M}}=\dfrac{Pe}{Pe+2}$
p	Maximum of IF	$\mathrm{g}(H,\theta_{\mathrm{M}})=\sqrt{\dfrac{Pe+2}{\pi}}\exp\left(-\dfrac{1}{Pe+2}\right)-\dfrac{Pe}{2}\mathrm{e}^{Pe}\mathrm{erfc}\left(\dfrac{Pe+1}{\sqrt{Pe+2}}\right)$

3 Nonlinear SSQ method

Let $\boldsymbol{a}=(K, Pe, T, T_{\mathrm{d}}, c_0)$ be vector of parameters. Let (t_k, y_k) be experimental response for $k=1, ..., m$. The objective function for nonlinear regression is then well known sum of squares

$$\mathrm{SSQ}(\mathbf{a})=\sum\left(K\,\mathrm{g}\left(\frac{t_k-T_d}{T}, Pe\right)+c_0-y_k\right)^2 \tag{7}$$

Let SSQ reaches its minimum value SSQ_{opt} in point $\boldsymbol{a}_{\mathrm{opt}}$. Let $\boldsymbol{H}=\partial^2\mathrm{SSQ}(\boldsymbol{a}_{\mathrm{opt}})/\partial\boldsymbol{a}^2$ be positive definite Hessian matrix in the maximum likelihood estimate. Now we can estimate the model error $s_{\mathrm{e}}=(SSQ_{\mathrm{opt}}/(m-n))^{1/2}$ and one-standard deviation of parameters as vector

$$\mathbf{s} = s_e \sqrt{\mathrm{diag}\left(2\mathbf{H}^{-1}\right)} \tag{8}$$

Here m is the number of experimental data and n is the number of estimated parameters. The last question is how to minimize the function SSQ in the neighborhood of the moment estimate.

Three aspects are necessary for the reliable optimization for non-convex functions

- The suitable domain of optimization, where the solution is expected
- The sophisticated initial estimate of searched parameters
- The effective method of convex optimization

In this specific case, the moment estimates were used as the initial parameter values. The optimization domain was created by 90 % decreasing, respectively increasing of the initial nominal values. The ***Predictioned conjugate gradient method*** was used for the task solution, because it is the recommended standard for the problems of this specific type. The Matlab realization of this method is well-known as `fmincon` function which attempts to find a constrained minimum of a scalar function of several variables starting at an initial estimate.

Table 5: AXIAL OPEN-OPEN MODEL PROPERTIES (AOO)

Item	Basic characteristics	Equation
a	Basic equation	$D_L \frac{\partial^2 c(x,t)}{\partial x^2} - u\frac{\partial c(x,t)}{\partial x} = \frac{\partial c(x,t)}{\partial t}$
b	Initial and boundary conditions	$c(x,0) = 0, \quad -\infty \le x \le \infty$ $x \to \pm\infty: \quad c(\pm\infty, t) = 0, t \ge 0$ $\lim_{x\to 0+} \frac{\partial c(x,t)}{\partial x} - \lim_{x \to 0-} \frac{\partial c(x,t)}{\partial x} = -\frac{u}{D_L} c_{in}(t)$
c	Transfer function	$G(H,p) = \frac{1}{a}\exp\left(\frac{Pe}{2}(1-a)\right), \quad a = \sqrt{1+\frac{4p\tau}{Pe}}, \quad \tau = H/u$
d	Impulse function (IF)	$g(H,\theta) = \frac{1}{2}\sqrt{\frac{Pe}{\pi\theta}}\exp\left(-\frac{Pe(1-\theta)^2}{4\theta}\right)$
e	Step response	$h(H,\theta) = \frac{1}{2}\left\{\mathrm{erfc}\left(\sqrt{\frac{Pe}{\theta}}\frac{1-\theta}{2}\right) - e^{Pe}\,\mathrm{erfc}\left(\sqrt{\frac{Pe}{\theta}}\frac{1+\theta}{2}\right)\right\}$
f	0^{th} raw moment of IF	$M_0^\theta = 1$
g	1^{st} raw moment of IF	$M_1^\theta = 1 + 2/Pe$
h	2^{nd} raw moment of IF	$M_2^\theta = 1 + 6/Pe + 12/Pe^2$
i	3^{rd} raw moment of IF	$M_3^\theta = 1 + 12/Pe + 60/Pe^2 + 120/Pe^3$
j	4^{th} raw moment of IF	$M_4^\theta = 1 + 20/Pe + 180/Pe^2 + 840/Pe^3 + 1680/Pe^4$
k	Dispersion, variance	$\sigma^2 = (2Pe+8)/Pe^2$
l	Coefficient of variation	$\gamma = \frac{\sqrt{2Pe+8}}{Pe+2}$
m	Skewness	$\gamma_1 = \sqrt{2}\frac{3Pe+16}{\sqrt{(Pe+4)^3}}$
n	Kurtosis	$\gamma_2 = \frac{192+30Pe}{(Pe+4)^2}$
o	Mode	$\theta_M = \frac{c-1}{Pe}, \quad c = \sqrt{1+Pe^2}$
p	Maximum of IF	$g(H,\theta_M) = \frac{Pe}{2\sqrt{\pi(c-1)}}\exp\left(\frac{Pe-c}{2}\right)$

One of the possible types of the function application is presented here as

`x = fmincon(fun,x0,A,b,Aeq,beq,lb,ub)`

where `x` is optimum parameter vector, `fun` is the name of the objective function, `x0` is the initial estimate vector, `lb` and `ub` are the lower, respectively upper bound on the optimization domain. The remaining parameters `A, b, Aeq, beq` represent the other linear constrains and there are empty in this specific task.

4 Experimental part

Experimental data of the residence time distribution (RTD) in liquid phase were measured in pilot plant trickle bed reactor. The main part of the reactor consisted of 1,5 m long stainless-steel column 0,1 m in diameter. Column was filled to the height of 1,5 m with 3mm spherical particles of commercial catalyst Noblyst 1505 (Degussa). Toluene and nitrogen were used as a model phase system. All experiments were conducted at pressure 0.3 MPa (abs.) and temperature 20 °C. Set of experimental data was done at liquid and gas superficial velocities: $v_L = 0.0035$ m/s and $v_G = 0.044$-0.178 m/s.

RTD in liquid phase was measured via impulse-response method, where tracer injected to the reactor was monitored by refractometer in the outlet stream. Isobutanol served as a suitable tracer which provides linear dependence of refractive index on isobutanol concentration in toluene. Refractive index was measured by digital refractometer PR-23 (K-Patents, Finland). This through-flow refractometer installed at reactor outlet and it didn't need extra sampling of liquid mixture. Thanks to built-in temperature sensor the device provided values of measured refractive index with temperature compensation. Measurable range of refractive index is $1.3100 \le n_D \le 1.5400$ with accuracy $n_D \pm 0.0002$ and sampling frequency 1 *Hz.* This range sufficiently covered measured values which varied between 1.3928 (isobutanol) and 1.4922 (toluene).

To minimize impact of tracer injection on flow pattern in the reactor, the tracer was injected at the same feed rate as liquid phase. Liquid phase feed was switched off during tracer injection which was 5 sec in all cases.

5 Results

For given experimental data the results of approximations via the four ADMs presented above are drawn up in Table 6. Only one data file is presented in this paper. For the other data files with various flows of liquid and gas the results are similar.

It was necessary to take account the transport delay T_d into the evaluation procedure of experimental data. This delay is a function of liquid and gas flow rate. It represents the time delay due to tracer transport of to the measured section. It wasn't possible to measure delay experimentally due to construction disposition of pilot plant apparatus and hence it was optimized as a model parameter. Optimum value of the delay was ca. 46 sec.

Evaluated value of Peclet number (from Table 6) is about 4 what indicates negligible extent of axial dispersion in the reactor for all ADMs.

The comparison of data approximation for all 4 ADMs is presented in Figure 3. Because the model errors are small, the curves nearly melt. So that, the details of the beginning, peak and tail part are presented in Figs. 4-6.

The relative error in the beginning part of the weighting function approximation for all ADMs is quite high (max. 75 %) because it depends on the quality of T_d estimate (the best is AEO model). The relative error in the peak part of the weighting function approximation is max. 6 % (the best is AOO model). The relative error in the tail part of experimental and approximation curves depends on the quality of data measurement and an elected model type (the best is for AEO model).

Table 6: EXAMPLE OF EVALUATED PARAMETERS OF ALL ADMS

parameter	estimate	AEO	ACO	ACC	AOO
K	moment	0.0068	0.0084	0.0079	0.0099
	LSQ	0.0076	0.0101	0.0079	0.0125
	SD	0.0000	0.0001	0.0001	0.0002
Pe	moment	4.9705	3.7887	1.9479	3.0336
	LSQ	4.2952	3.6356	3.0286	3.7462
	SD	0.1315	0.1165	0.1212	0.1136
T (s)	moment	66.4556	49.1076	55.6017	34.0959
	LSQ	56.1531	41.9588	53.3562	33.6796
	SD	0.3584	0.4008	0.3515	0.4473
Td (s)	moment	36.5733	53.9212	47.4271	68.9329
	LSQ	44.9167	46.9730	46.6234	48.0486
	SD	0.3778	0.3807	0.4084	0.3730
model error		1.73E-04	1.71E-04	1.73E-04	1.71E-04

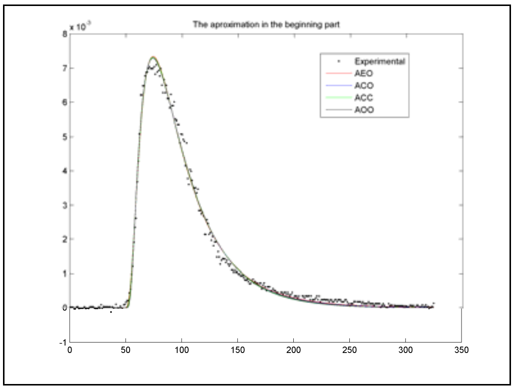

Figure 3: The data approximation for 4 models

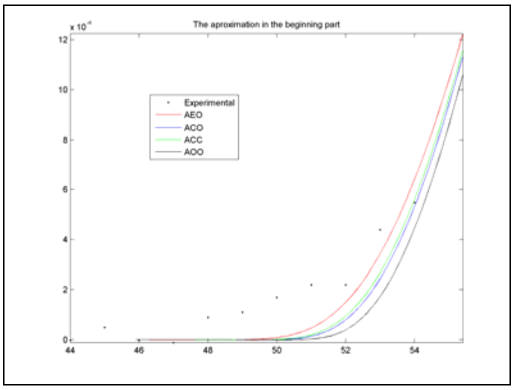

Figure 4: The data approximation for 4 models in the start part of characteristics

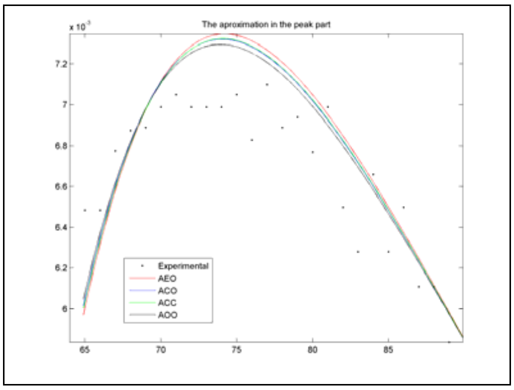

Figure 5: The data approximation for 4 models in the peak part of characteristics

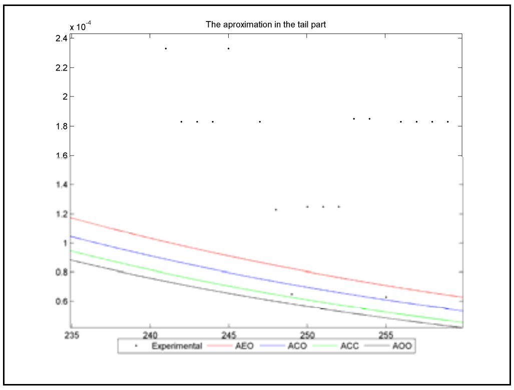

Figure 6: The data approximation for 4 models in the tail part of characteristics

6 Conclusion

All ADMs fit the given experimental data well. The model election depends on the criterion of the optimization as it is shown here.

- In case the criterion of the optimization is the minimal model general error then ACO and AOO models are the best ones.
- In case the criterion of the optimization is the value of the transport delay T_d then ACC model is the best. But this model has a lot of disadvantages – the model evaluation takes more than 8 hours (in normal PC) for given data (because of complicated sum evaluation).

- In case the criterion of the optimization is the model complexity then AOO model is the best one (it is the simplest model).
- In case the criterion of the optimization is the time of model evaluation then AEO and AOO models are the best ones, because the evaluation time is the shortest (less then 5 minutes).
- In case the criterion of the optimization is the relative error of approximation in the beginning part of the weighting function then AEO model is the best, for the relative error of curve approximation in the peak part AOO is the best model and for the tail part AEO model is the best one.

7 Acknowledgement

This work has been supported by the Ministry of Education of the Czech Republic, program No. MSMT 6046137306

8 List of Symbols

a – vector of parameters (K, Pe, T, T_d, c_0)
c(x, t) – tracer concentration (kg m^{-3})
D_L – coefficient of axial dispersion (m^2 s^{-1})
G(H, p) – transfer function
g(H, θ)– impulse function
H – tube length (m)
h(H, θ) – step response
M_k^θ – dimensionless k-th raw moment
n_D – refractive index
Pe – Peclet number (dimensionless)
Q_V – volumetric rate (m^3 s^{-1})
s_e – one-standard deviation of parameters
SSQ – function for sum of squares evaluation
t – time (s)
T_d – transport delay (s)
u – velocity of convective flow (m s^{-1})
u_b – velocity of back current (m s^{-1})
V – volume (m^3)
x – length coordinate (m)
v_G – gas velocity (m s^{-1})
v_L – liquid velocity (m s^{-1})

γ – coefficient of variation
γ_1 – skewness
γ_2 – kurtosis
θ – dimensionless time $\theta = t/\tau$
κ – roots of transcendent equation
μ_k – dimensionless k^{th} central moment
σ^2 – variance
$\tau = T$ – mean residence time (s)

ACC – axial closed-closed model
ACO – axial closed-open model
AEO – axial enforced closed-open model
AOO – axial open-open model
ADM – axial dispersion model
RTD – residence time distribution
TBR – trickle bed reactor
LSQ – least square method
SD – standard deviation

References

[1] Dudukovic, M. P., F. Larachi, et al. (1999). *Multiphase reactors – revisited*. Chemical Engineering Science 54 (13-14), 1999, pp. 1975-1995.

[2] Westerterp, K. R., Wammes, W. J. A. *Three-Phase Trickle-Bed Reactors*. Ullmann's Encyclopedia of Industrial Chemistry. Weinheim, Wiley-VCH Verlag GmbH, 2008

[3] Fodor, G. *Laplace Transforms in Engineering*. Académiai Kiadó, Budapest, 1965

[4] Himmelblau, D., Bischoff, K. B. *Process Analysis and Simulation –Deterministic Systems.* John Wiley and Sons, Inc., New York, 1968

[5] Wen, C.Y., Fan, L. T. *Models for Flow Systems and Chemical Reactors.* Marcel Dekker, Inc., New York, 1975

[6] Čermáková, J., Scargiali, F., Siyakatshana, N., Kudrna, V., Brucato, A., Machoň, V. *Axial dispersion model for solid flow in liquid suspension in system of two mixers in total recycle.* Chemical Engineering Journal, Vol. 117, Issue 2, April 2006, pp. 101-107

[7] Coleman, T. F., Verma, A. *A predictioned conjugate gradient approach to linear equality constrained minimization*. Computational Optimization and Applications, 20 (1), 2001, pp. 61-72

[8] Kudrna, V., Jahoda, M., Siyakatshana, N., Čermáková, J., Machoň, V. *General solution of the dispersion model for a one-dimensional stirred flow system using Danckwerts' boundary conditions*. Chemical Engineering Science, Vol. 59, Issue 14, July 2004, pp. 3013-3020

[9] Levenspiel, O., Smith, W. K. *Notes on the diffusion-type model for the longitudinal mixing of fluids in flow*. Chemical Engineering Science, 1957, Vol. 6, No. 4-5, pp. 227-233

[10] Martin, A. D. *Interpretation of residence time distribution data*. Chemical Engineering Science, 2000, Vol. 55, No. 23 (December), 5907-5917

[11] Sorensen, D. C. *Minimization of a Large Scale Quadratic Function Subject to an Ellipsoidal Constraint*. Department of Computational and Applied Mathematics, Rice University, Technical Report TR94-27, 1994.

Darina Bártová

Institute of Chemical Technology, Department of Computing and Control Engineering, Technická 5, 166 28 Prague 6, tel.: +420 220 444 170, e-mail: dbartova@vscht.cz